

ChemComm

Accepted Manuscript



This is an *Accepted Manuscript*, which has been through the Royal Society of Chemistry peer review process and has been accepted for publication.

Accepted Manuscripts are published online shortly after acceptance, before technical editing, formatting and proof reading. Using this free service, authors can make their results available to the community, in citable form, before we publish the edited article. We will replace this *Accepted Manuscript* with the edited and formatted *Advance Article* as soon as it is available.

You can find more information about *Accepted Manuscripts* in the [Information for Authors](#).

Please note that technical editing may introduce minor changes to the text and/or graphics, which may alter content. The journal's standard [Terms & Conditions](#) and the [Ethical guidelines](#) still apply. In no event shall the Royal Society of Chemistry be held responsible for any errors or omissions in this *Accepted Manuscript* or any consequences arising from the use of any information it contains.



ChemComm

COMMUNICATION

Insights into N-doping in single-walled carbon nanotubes for enhanced activation of superoxides: a mechanistic study

Received 00th January 2015,
Accepted 00th January 2015

Xiaoguang Duan,^a Zhimin Ao,^b Hongqi Sun,^{*a} Li Zhou,^a Guoxiu Wang,^b and Shaobin Wang^{*a}

DOI: 10.1039/x0xx00000x

www.rsc.org/

Emerging characteristics upon nitrogen-doping was differentiated in activation of superoxides over single-walled carbon nanotubes. Both experimental and theoretical studies revealed that enhanced peroxymonosulfate (PMS) activation is ascribed to a nonradical process while persulfate (PS) activation is accelerated via directly oxidizing water, yet hydrogen peroxide (H₂O₂) activation is inert to N-doping. This study dedicates the first insights into versatile N-doping in carbocatalysis for organic oxidation in sustainable remediation.

In recent years, water pollution has become one of the key issues in environmental deterioration which triggers worldwide concerns. Sustainable water resources from domestic sewage and industrial wastewater can be exploited through advanced oxidative processes (AOPs). Various superoxides such as ozone (O₃), hydrogen peroxide (H₂O₂), persulfate (S₂O₈²⁻, PS), and peroxymonosulfate (HSO₅⁻, PMS) are activated to produce reactive radicals to decompose toxic organic compounds into carbon dioxide, water and mineralized acids. For example, conventional Fenton reactions employ ferrous ions as an efficient homogeneous catalyst to activate H₂O₂ to generate hydroxyl radicals. However, this process requires strict acidic condition (pH~3) and produces a lot of sludge due to coagulation.¹ Metal-based heterogeneous catalysts, such as MnO₂,² CuO,³ CuFe₂O₄,⁴ and zerovalent iron (ZVI),⁵ have been used to activate PMS and PS to conduct sulfate radical based oxidation, yet the stubborn toxic metal leaching severely limits the future practical applications.

Emerging carbocatalysis is able to completely avoid the secondary contamination from the metal leaching owing to its metal-free nature.^{6, 7} However, the efficiencies of pristine nanocarbons in activation of superoxides are very low. We first discovered that reduced graphene oxide (rGO) can effectively activate PMS and further proved that nitrogen doping can remarkably enhance the

catalytic oxidation.^{8, 9} Heteroatom doping can effectively break the inertness of graphene carbon matrix and induce novel physicochemical and electronic properties for enhanced catalysis.¹⁰⁻¹⁵ More recently, we observed that nitrogen-doping would induce a non-radical pathway in catalytic oxidation with PMS.^{16, 17} However, the origin of the emerging features from nitrogen doping is not clear in PMS activation yet, and even more blurred in PS and H₂O₂ activation.

In this study, experimental results and theoretical calculations are integrated to reveal the effect of nitrogen doping on the radical generation processes over single-walled carbon nanotubes (SWCNTs). The pristine SWCNTs were thoroughly refluxed in concentrated nitric acid to remove any potential metal impurities (denoted as o-SWCNT). The purified o-SWCNT was then heated at 700 °C in N₂ to remove excess functional groups (denoted as SWCNT-700), or annealed with melamine as a N-precursor to produce nitrogen-doped sample (denoted as N-SWCNT).¹⁷ The physical and chemical properties of prepared carbocatalysts are displayed in Table S1 (ESI†). The nitrogen modified SWCNTs were designed with a highly crystallized structure (I_D/I_G=0.35) and a low oxygen level (1.15 at.%) to minimize the system complexity from defects and functional groups. Effect of nitrogen doping on activation of PMS, PS, and H₂O₂ was evaluated by phenol oxidation. Fig. 1 shows that the super-oxidants can hardly oxidize phenol without a catalyst. The catalytic performance of the modified SWCNTs for PMS activation is illustrated in Fig. 1a. The o-SWCNT can provide 56.5% phenol removal in 180 min, while SWCNT-700 and N-SWCNT achieved complete phenol degradation in 180 and 45 min, respectively.¹⁷ The initial reaction rates of o-SWCNT, SWCNT-700, and NoCNT were calculated to be 0.09, 0.46, and 4.93 ppm•min⁻¹, respectively, based on pseudo first-order kinetics. The observations on carbon nanotubes-based materials were consistent with those of rGO, which is more efficient for PMS activation than GO with excess oxygen groups but less active than nitrogen doped rGO.^{8, 9, 16} We further combined experimental design and computational studies to reveal that substitutional N-doping (graphitic N) can effectively break the chemical inertness of conjugated graphene network and facilitate charge transfer from adjacent carbon atoms to graphitic nitrogen atoms, giving rise to positively charged sites which can effectively improve the adsorption capability of PMS and weaken the O-O (HO-SO₄)

^a Department of Chemical Engineering, Curtin University, GPO Box U1987, Perth, WA 6845, Australia. E-mail: Shaobin.wang@curtin.edu.au (S.W.), h.sun@curtin.edu.au (H.S.)

^b Centre for Clean Energy Technology, School of Mathematical and Physical Sciences, University of Technology Sydney, PO Box 123, Broadway, Sydney, NSW 2007, Australia

† Electronic Supplementary Information (ESI) available: [EPR spectra, theoretical calculation details]. See DOI: 10.1039/x0xx00000x

bond.^{16, 18} The influence of annealing temperature of N-SWCNTs on PS activation was illustrated in Fig. S2 (ESI†). N-SWCNTs obtained at 700 °C present the best catalytic activity, which is well consistent with our previous studies on PMS activation on N-rGO and N-SWCNT.^{16, 17} Raising temperature results in a lower N concentration owing to the breakup of C-N bonds, meanwhile attaining a higher graphitic N proportion due to its better thermal stability. The experimental results suggest that both N-doping level and nitrogen species synergistically affect the carbocatalysis for peroxide activation. Additionally, the stability of the carbocatalysts was evaluated as shown in Fig. S3 (ESI†). The N-SWCNTs in the 2nd and 3rd cycles provided 73.2% and 53.0% phenol removal, respectively. The deactivation of the carbocatalysts can be ascribed to the alteration of surface charges and the detachment of N dopants during the oxidation processes.

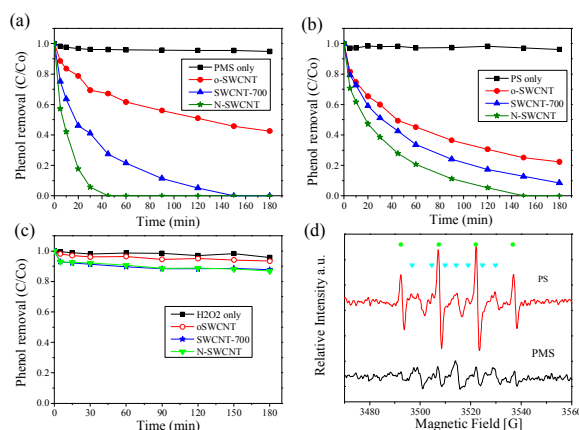


Fig. 1 Phenol oxidation with (a) PMS (6.5 mM), (b) PS (6.5 mM) and (c) H₂O₂ (30 mM) under various conditions. [Phenol] = 20 ppm, [Catalyst] = 0.1 g/L, [Temperature] = 25 °C. (d) EPR spectra of PMS and PS activation on N-SWCNT (●: DMPO-OH, ♥: DMPO-SO₄).

N-doping for potentially enhanced PS and H₂O₂ activation is presented in Figs. 1b and c. It was found that N-doping can slightly improve the catalytic performance in PS activation, however, is ineffective for H₂O₂ activation. More specifically, o-SWCNT, SWCNT-700, and N-SWCNT attained 77.8, 91.6, and 100% phenol degradation with PS in 180 min and the initial reaction rates were estimated to be 0.32, 0.42, and 0.60 ppm·min⁻¹ accordingly. It is interesting to note that, though o-SWCNT is more efficient for PS activation than PMS, nitrogen-doped sample does not show the same trend, suggesting that the intrinsic mechanism of PS and PMS activation on N-SWCNT might be different. Fig. 1c indicates poor effectiveness for H₂O₂ activation on both SWCNT-700 and N-SWCNT with only 12.3 and 13.1% phenol oxidation in 180 min, compared with 6.7% phenol removal on o-SWCNT. Recently, Yang et al. reported that ozone can react with PMS to generate sulfate and hydroxyl radicals,¹⁹ which motivated us to explore if such a synergistic effect exists in the PMS/H₂O₂ or PS/H₂O₂ systems. However, as illustrated in Fig. S4 (ESI†), we found that both PMS and PS cannot work as efficient initiators to improve the activation of H₂O₂ on N-SWCNT. Moreover, the presence of H₂O₂ lowered the phenol oxidation efficiency on PMS/N-SWCNT and PS/N-SWCNT. We employed *in-situ* electron paramagnetic resonance (EPR) to investigate the radical generation process during PMS and PS activation on the carbocatalysts. As the generated free radicals

usually have a very short lifetime and then quickly react with the organic compounds or are quenched through coupling with another radical molecule, the free-radicals were captured by a spin-trapping agent, 5,5-dimethyl-1-pyrroline N-oxide (DMPO), to form relative stable adducts and detected by EPR for the mechanistic study. As illustrated in Fig. 1d and Fig. S5 (ESI†), N-SWCNT can activate both PMS and PS to generate sulfate radicals (SO₄^{•-}) and hydroxyl radicals (•OH). Nevertheless, the PMS/N-SWCNT system is much more efficient than PS/N-SWCNT for phenol oxidation, the intensity of generated radicals from PS activation is much higher than that from PMS. In the AOPs, the reactive radicals play crucial roles in attacking and decomposing organics into oxidated products. The intrinsic distinction of PMS and PS activation on N-SWCNTs for radical generation and phenol oxidation implies the completely different reaction pathways.

Table 1. The adsorption energy E_{ads} , electrons transfer between SWCNT and the adsorbed molecule Q , and the O-O bond length ($l_{\text{O-O}}$) of SO₃-OH in PMS, SO₄-SO₄ in PS, and HO-OH in H₂O₂ from different adsorption configurations in Fig. S6 (ESI†).

Type of CNT	Molecules	E_{ads} (eV)	Q (e)	$l_{\text{O-O}}$ (Å)
Free molecule	PMS	-	-	1.326
	PS	-	-	1.222
	H ₂ O ₂	-	-	1.471
SWCNT	PMS	-2.05	-0.455	1.402
	PS	-1.74	-0.693	1.295
	H ₂ O ₂	-0.30	0	1.469
N-doped SWCNT	PMS	-2.98	-0.757	1.459
	PS	-2.99	-0.945	1.344
	H ₂ O ₂	-0.26	0.007	1.471

We further carried out density functional theory (DFT) calculations to discover the intricate interactions between the superoxides and carbocatalysts. The corresponding O-O bond lengths ($l_{\text{O-O}}$) in free PMS, H₂O₂ and PS are 1.326, 1.471, and 1.222 Å, respectively. Table 1 suggests that the adsorption of PMS and PS on both SWCNT and N-doped SWCNT is quite strong, which induces relatively large electron transfer between the oxidant molecules and SWCNT (or N-SWCNT). The O-O bond length ($l_{\text{O-O}}$) of SO₃-OH in PMS and SO₄-SO₄ in PS increased remarkably comparing with that of free PMS and PS. However, the adsorption of H₂O₂ is very weak, mirrored by the low adsorption energy and near zero charge transfer. Therefore, SWCNT is theoretically proven to have excellent performance to activate PMS and PS molecules to be dissociated into -SO₃ and -OH groups, or two -SO₄ groups. The noticeable electron transfer tendency (Q) possibly suggests the generation of free radicals and anions. After N incorporation into SWCNT, the catalytic performance increases with a higher adsorption energy, more rapid charge transfer, and larger $l_{\text{O-O}}$ value. Such changes were not observed in H₂O₂ activation. Thus, the theoretical calculations were in well accordance with the experimental results.

Nevertheless the calculations revealed that nitrogen doping has a more remarkable enhancement for PS activation than PMS (reflected by more significant increases in E_{ads} , Q , and $l_{\text{O-O}}$), the catalytic oxidation did not follow this theoretical expectation. Based on the experiments and DFT calculations, we suggest that PMS and PS activation processes on N-SWCNT might be different. In a previous study, we first discovered that N-doping can induce nonradical reactions which co-exist with the radical pathway during catalytic

phenol oxidation with PMS.¹⁷ The PMS molecules are first adsorbed and interacted with activated sp^2 -conjugated carbon network due to nitrogen-doping, and then reacted rapidly with the target organics via a nonradical-generated oxidation process. The same phenomenon was also found in a PS/CuO system. PS first interacts with the outer-sphere of CuO electronic shell, which is the rate-limiting step, and then decomposes 2, 4-chlorophenol directly.³ In order to investigate if such non-radical processes occur in the PS/N-SWCNT system as well, ethanol (EtOH), which can quickly quench both the sulfate and hydroxyl radicals, was utilized as a radical scavenger to quench the reactive species produced from PS activation.²⁰ The phenol degradation efficiency decreased significantly with the rising ratio of ethanol in PS/SWCNT-700 and PS/N-SWCNT systems (Figs. 2a and b). The initial reaction rates were estimated (Fig. 2c) and reduced significantly when the water was completely replaced by ethanol (only around 1% water remaining introduced during preparation of phenol solution), which is intrinsically different from the PMS/N-SWCNT system in which very high phenol removal efficiency still maintained in the ethanol solution.¹⁷ The oxidation reaction was almost terminated at high concentration of ethanol in PS/N-SWCNT systems, suggesting that the generation of reactive radicals was essential for phenol oxidation with PS and non-radical process was almost absent in the PS/N-SWCNT system.

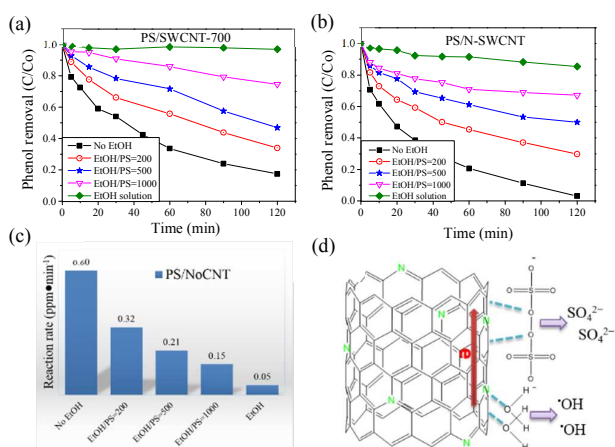


Fig. 2 Effects of radical scavenger (EtOH) on phenol degradation in (a) PS/SWCNT-700, and (b) PS/N-SWCNT systems. (c) Reaction rates of phenol oxidation with PS on N-SWCNT under different ratios of EtOH. ([Phenol] = 20 ppm, [Catalyst] = 0.1 g/L, [Temperature] = 25 °C, [PS]=6.5 mM.) (d) Proposed mechanism of PS activation on N-SWCNT.

It is also noteworthy that N-SWCNT can effectively activate PS to generate large amounts of hydroxyl radicals ($\cdot\text{OH}$) as indicated in the EPR spectra (Fig. 1d). To the best of our knowledge, persulfate ($\text{S}_2\text{O}_8^{2-}$) cannot generate hydroxyl radicals itself and the large amounts of hydroxyl radicals can exclusively be devolved from water. We suppose that PS might be able to oxidize water directly on N-SWCNT to generate hydroxyl radicals for phenol degradation, shown in Fig. 2d. A theoretical model was built up to modulate this process as presented in Figs. 3a and b. As one can see from Fig. 3c and Table S2 (ESI†), the adsorption of H_2O molecules on nitrogen-doped SWCNT is minor due to the weak adsorption energy, little electron transfer from H_2O to SWCNT, and the O-H bond length

rarely changes after adsorption. However, if a PS molecule presents together with a water molecule on the N-SWCNT (Fig. 3b), the H_2O molecule adsorption enhances remarkably, where the adsorption energy increases by almost 3 times, the charge transfer becomes 7 times more faster, and the O-H bond length is also prolonged greatly (Table S2 ESI†). The adsorption capability of PS is also enhanced with a longer O-O bond length and faster electron transfer (Fig. 3d). Therefore, the presence of PS can promote the dissociation of H_2O and facilitate the generation of $\cdot\text{OH}$ group to form hydroxyl radicals. N-doped carbon nanotubes can activate H_2O molecules via acting as a fascinating bridge for electron transfer from H_2O to PS as proposed in Fig. 2d. Besides, PS might be converted into sulfate ions directly due to its great ability to extract electrons from the carbon matrix on N-SWCNT (Fig. 3d and Table S2, ESI†) when it co-exists with adsorbed water, as no obvious signal of sulfate radicals can be found in EPR spectra in Fig. 1d. Distinct from PS and H_2O_2 , the asymmetric structure of PMS (HO-SO_4) and the relative weak adsorption and oxidation ability on N-SWCNT might contribute to the emerging nonradical reaction for PMS activation.

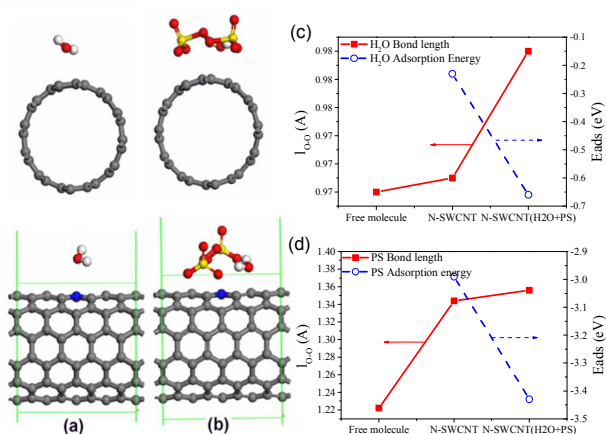


Fig. 3 (a) H_2O adsorption on N-SWCNT, (b) PS and H_2O adsorbed on the N-SWCNT. (The grey, blue, red, yellow, and white atoms are C, N, O, S, and H atoms, respectively. The O-O bond length ($l_{\text{O-O}}$) and adsorption energy of (c) H_2O and (d) PS under different conditions: free molecule, adsorption alone on N-SWCNT, and co-adsorbed on N-SWCNT.

In summary, we investigated the effect of N-doping on activation of various superoxides including PMS, PS, and H_2O_2 . Both experimental results and theoretical calculations proved that N-doping can enhance PMS and PS activation, yet is not effective for H_2O_2 activation. N-doping can induce nonradical oxidation in PMS activation, whereas works as an excellent electron-bridge to facilitate PS to oxidize adsorbed water to generate hydroxyl radicals for catalytic oxidation. This study concludes new insights into N-doping in carbocatalysis for oxidative processes in aqueous phase.

This work was financially supported by Australian Research Council under project No. DP130101319. Computational study was supported by the National Computational Infrastructure (NCI) through the merit allocation scheme and used NCI resources and facilities in Canberra, Australia. H. S. acknowledges Curtin Research Fellowship and opening project (KL-13 02).

Notes and references

1. X. W. Liu, X. F. Sun, D. B. Li, W. W. Li, Y. X. Huang, G. P. Sheng and H. Q. Yu, *Water Res.*, 2012, **46**, 4371-4378.
2. E. Saputra, S. Muhammad, H. Sun, H. M. Ang, M. O. Tade and S. Wang, *Environ. Sci. Technol.*, 2013, **47**, 5882-5887.
3. T. Zhang, Y. Chen, Y. Wang, J. Le Roux, Y. Yang and J.-P. Croué, *Environ. Sci. Technol.*, 2014, **48**, 5868-5875.
4. T. Zhang, H. Zhu and J.-P. Croue, *Environ. Sci. Technol.*, 2013, **47**, 2784-2791.
5. P. Drzewicz, L. Perez-Estrada, A. Alpatova, J. W. Martin and M. G. El-Din, *Environ. Sci. Technol.*, 2012, **46**, 8984-8991.
6. W. Cui, Q. Liu, N. Y. Cheng, A. M. Asiri and X. P. Sun, *Chem. Commun.*, 2014, **50**, 9340-9342.
7. N. Y. Cheng, Q. Liu, J. Q. Tian, Y. R. Xue, A. M. Asiri, H. F. Jiang, Y. Q. He and X. P. Sun, *Chem. Commun.*, 2015, **51**, 1616-1619.
8. H. Q. Sun, S. Z. Liu, G. L. Zhou, H. M. Ang, M. O. Tade and S. B. Wang, *ACS Appl. Mater. Interfaces*, 2012, **4**, 5466-5471.
9. H. Q. Sun, Y. X. Wang, S. Z. Liu, L. Ge, L. Wang, Z. H. Zhu and S. B. Wang, *Chem. Commun.*, 2013, **49**, 9914-9916.
10. Y. Kim and S. Shanmugam, *ACS Appl. Mater. Interfaces*, 2013, **5**, 12197-12204.
11. J. Sanetuntikul, T. Hang and S. Shanmugam, *Chem. Commun.*, 2014, **50**, 9473-9476.
12. Z.-S. Wu, S. Yang, Y. Sun, K. Parvez, X. Feng and K. Muellen, *J. Am. Chem. Soc.*, 2012, **134**, 9082-9085.
13. Y. Li, Y. Zhao, H. Cheng, Y. Hu, G. Shi, L. Dai and L. Qu, *J. Am. Chem. Soc.*, 2012, **134**, 15-18.
14. S. Y. Wang, L. P. Zhang, Z. H. Xia, A. Roy, D. W. Chang, J. B. Baek and L. M. Dai, *Angew. Chem. Int. Ed.*, 2012, **51**, 4209-4212.
15. J. Liang, Y. Jiao, M. Jaroniec and S. Z. Qiao, *Angew. Chem. Int. Ed.*, 2012, **51**, 11496-11500.
16. X. G. Duan, Z. M. Ao, H. Q. Sun, S. Indrawirawan, Y. X. Wang, J. Kang, F. L. Liang, Z. H. Zhu and S. B. Wang, *ACS Appl. Mater. Interfaces*, 2015, **7**, 4169-4178.
17. X. G. Duan, H. Q. Sun, Y. X. Wang, J. Kang and S. B. Wang, *ACS Catal.*, 2015, **5**, 553-559.
18. X.G. Duan, K. O'Donnell, H. Q. Sun, Y. X. Wang and S. B. Wang, *Small*, 2015, **11**, 3036-3044.
19. Y. Yang, J. Jiang, X. L. Lu, J. Ma and Y. Z. Liu, *Environ. Sci. Technol.*, 2015, **49**, 7330-7339.
20. G. P. Anipsitakis and D. D. Dionysiou, *Environ. Sci. Technol.*, 2003, **37**, 4790-4797.